scientific reports

OPEN

Ocean dynamic equations with the real gravity

Peter C. Chu

Two different treatments in ocean dynamics are found between the gravity and pressure gradient force. Vertical component is 5–6 orders of magnitude larger than horizontal components for the pressure gradient force in large-scale motion, and for the gravity in any scale motion. The horizontal pressure gradient force is considered as a dominant force in oceanic motion from planetary to small scales. However, the horizontal gravity is omitted in oceanography completely. A non-dimensional C number (ratio between the horizontal gravity and the Coriolis force) is used to identify the importance of horizontal gravity in the ocean dynamics. Unexpectedly large C number with the global mean around 24 is obtained using the community datasets of the marine geoid height and ocean surface currents. New large-scale ocean dynamic equations with the real gravity are presented such as hydrostatic balance, geostrophic equilibrium, thermal wind, equipotential coordinate system, and vorticity equation.

Gravity is greatly simplified in oceanography from a three-dimensional vector field [$\mathbf{g} = (g_\lambda, g_\varphi, g_z)$] with (λ, φ, z) being the (longitude, latitude, height) and $(\mathbf{i}, \mathbf{j}, \mathbf{k})$ being the corresponding unit vectors with eastward positive for $\mathbf{i}$, northward positive for $\mathbf{j}$, and upward positive (in the Earth radial direction) for $\mathbf{k}$ to a vertical vector ($-g_0\mathbf{k}$) with the uniform gravity $g_0 = 9.81$ m/s². The feasibility of such a practice has never been challenged because the horizontal components (g_λ, g_φ) are much smaller (5–6 orders of magnitudes) than the vertical component g_z and the deviation of the magnitude of g_z to g_0 is also very small. However, similar situation also occurs with the three-dimensional pressure gradient force: the horizontal pressure gradient force is much smaller (5–6 orders of magnitudes) than the vertical pressure gradient force in large-scale oceanic motion. The horizontal pressure gradient forces are considered important in oceanic motion for any scales. Thus, the feasibility to neglect the horizontal gravity components (g_λ, g_φ) against the vertical gravity (g_z) needs to be investigated. The correct approach is to compare the horizontal gravity with the horizontal forces such as the Coriolis force or the horizontal pressure gradient force.

Reference coordinate systems. The polar spherical coordinates (more popular) and oblate spherical coordinates (less popular, see Appendix) are the reference coordinate system used in the Earth science. In all the fields of the Earth science such as meteorology, oceanography, and geodesy, the horizontal component of any vector **A** is on the spherical surface if the polar spherical coordinates are used or on the ellipsoidal surface if the oblate spherical coordinates are used,

$$\mathbf{A} = \mathbf{A}_h + A_z\mathbf{k}, \ \mathbf{A}_h = A_\lambda\mathbf{i} + A_\varphi\mathbf{j} \tag{1}$$

no matter the variable is evaluated on the geoid, isobaric, isopycnal, or topographic-following surfaces. Ocean numerical models have several representations of the vertical (i.e., the radial) coordinate such as z-coordinate[1,2], isopycnal coordinate[3,4], topographic-following coordinate (i.e., sigma-coordinate)[5,6]. However, the horizontal component of the vector **A** is always given by (1).

Three forms of the gravity. Three forms of gravity exist in geodesy and oceanography: the real gravity $\mathbf{g}(\lambda, \varphi, z)$, the normal gravity [$-g(\varphi)\mathbf{k}$], and the uniform gravity ($-g_0\mathbf{k}$, $g_0 = 9.81$ m/s²). The real gravity (**g**) is a three-dimensional vector field, which is decomposed into

$$\mathbf{g} = \mathbf{g}_h + g_z\mathbf{k}, \ \mathbf{g}_h = g_\lambda\mathbf{i} + g_\varphi\mathbf{j} \tag{2}$$

where $\mathbf{g}_h$ is the horizontal gravity component; and ($g_z\mathbf{k}$) is the vertical gravity component. The normal gravity vector [$-g(\varphi)\mathbf{k}$] (vertical vector) is associated with a mathematically modeled Earth (i.e., a rigid and geocentric ellipsoid) called the normal Earth. The normal Earth is a spheroid (i.e., an ellipsoid of revolution), has the same total mass and angular velocity as the Earth, and coincides its minor axis with the mean rotation of the Earth[7].

Department of Oceanography, Naval Postgraduate School, Monterey, CA, USA. email: pcchu@nps.edu

Similar to $\mathbf{g}(\lambda, \varphi, z)$, the normal gravity $[-g(\varphi)\mathbf{k}]$ is the sum of the gravitational and centrifugal accelerations exerted on the water particle by the normal Earth. Its intensity $g(\varphi)$ is called the normal gravity and determined analytically. For example, the World Geodetic System 1984 uses the Somiglina equation to represent $g(\varphi)$[8]

$$g(\varphi) = g_e \left[\frac{1 + \kappa \sin^2 \varphi}{\sqrt{1 - e^2 \sin^2 \varphi}} \right], \; e^2 = \frac{a^2 - b^2}{a^2}, \kappa = \frac{bg_p - ag_e}{ag_e} \tag{3}$$

where (a, b) are the equatorial and polar semi-axes; a is used for the Earth radius, $R = a = 6.3781364 \times 10^6$ m; $b = 6.3567523 \times 10^6$ m; e is the spheroid's eccentricity; $g_e = 9.780$ m/s^2, is the gravity at the equator; and $g_p = 9.832$ m/s^2 is the gravity at the poles. The uniform gravity $(-g_0\mathbf{k})$ is commonly used in oceanography.

Real and normal gravity potential. Let (P, Q) be the Newtonian gravitational potential of the (real Earth, normal Earth) and P_R $(= \Omega^2 r^2 \cos^2 \varphi/2))$ be the potential of the Earth's rotation. Let $V = P + P_R$ be the gravity potential of the real Earth (associated with real gravity $\mathbf{g}$) and $E = Q + P_R$ be the gravity potential of the normal Earth [associated with the normal gravity $-g(\varphi)\mathbf{k}$]. The potential of the normal gravity $[-g(\varphi)\mathbf{k}]$ is given by

$$E(\varphi, z) = -g(\varphi)z \tag{4}$$

The gravity disturbance is the difference between the real gravity $\mathbf{g}(\lambda, \varphi, z)$ and the normal gravity $[-g(\varphi)\mathbf{k}]$ at the same point[9]. The potential of the gravity disturbance (called the disturbing gravity potential) is given by

$$T = V - E = P - Q. \tag{5}$$

Consequently, the centrifugal effect disappears and the disturbing gravity potential (T) can be considered a harmonic function. With the disturbing gravity potential T, the real gravity $\mathbf{g}$ $(= \mathbf{g}_h + g_z\mathbf{k})$ is represented by

$$\mathbf{g}_h = \nabla_h T, \; g_z = -g(\varphi) + \frac{\partial T}{\partial z} \tag{6}$$

where ∇_h is the horizontal vector differential operator. The geoid height relative to the normal Earth (i.e., reference spheroid) is given by Bruns' formula[10]

$$N(\lambda, \varphi) = \frac{T(\lambda, \varphi, 0)}{g_0} \tag{7}$$

Equations (5), (6), (7) clearly show that the fluctuation of the marine geoid is independent of the Earth rotation and dependent on the disturbing gravity potential (T) evaluated at $z = 0$ only.

The disturbing static gravity potential (T) outside the Earth masses in the spherical coordinates with the spherical expansion is given by[11]

$$T(r, \lambda, \varphi) = \frac{GM}{r} \sum_{l=2}^{\infty} \sum_{m=0}^{l} \left(\frac{R}{r} \right)^l \left[\left(C_{l,m} - C_{l,m}^{el} \right) \cos m\lambda + S_{l,m} \sin m\lambda \right] P_{l,m}(\sin \varphi), \tag{8}$$

where $G = 6.674 \times 10^{-11} \text{m}^3\text{kg}^{-1} \text{ s}^{-2}$, is the gravitational constant; $M = 5.9736 \times 10^{24}$ kg, is the mass of the Earth; r is the radial distance with $z = r - R$; $P_{l,m}(\sin \varphi)$ are the Legendre associated functions with (l, m) the degree and order of the harmonic expansion; $(C_{l,m}, C_{l,m}^{el}, S_{l,m})$ are the harmonic geopotential coefficients (Stokes parameters with $C_{l,m}^{el}$ belonging to the reference ellipsoid.

From Eqs. (4) and (5) the potential of the real gravity is given by

$$V = T - g(\varphi)z. \tag{9}$$

From Eq. (6) the real gravity is represented by

$$\mathbf{g}(\lambda, \varphi, z) = \nabla_h T + \left[\frac{\partial T}{\partial z} - g(\varphi) \right] \mathbf{k} \tag{10}$$

The horizontal gravity component at the reference ellipsoid surface $(z = 0)$ is obtained using (7) and (10)[12,13]

$$\mathbf{g}_h(\lambda, \varphi, 0) = \nabla_h T = g_0 \nabla_h N \tag{11}$$

An approximate 3D gravity field for oceanography. According to Eq. (8) (i.e., the spectral of the disturbing static gravity potential T), the ratio between $T(\lambda, \varphi, z)$ to $T(\lambda, \varphi, 0)$ through the water column can be roughly estimated by

$$\left| \frac{T(\lambda, \varphi, z)}{T(\lambda, \varphi, 0)} \right| \approx \frac{R}{(R + z)} \approx 1, \quad 0 \geq z \geq -H(\lambda, \varphi) \tag{12}$$

where H is the water depth. Since R is the radius of the Earth and more than 3 orders of magnitude larger than the water depth H. This leads to the first approximation that the surface disturbing gravity potential $T(\lambda, \varphi, 0)$ is used for the whole water column,
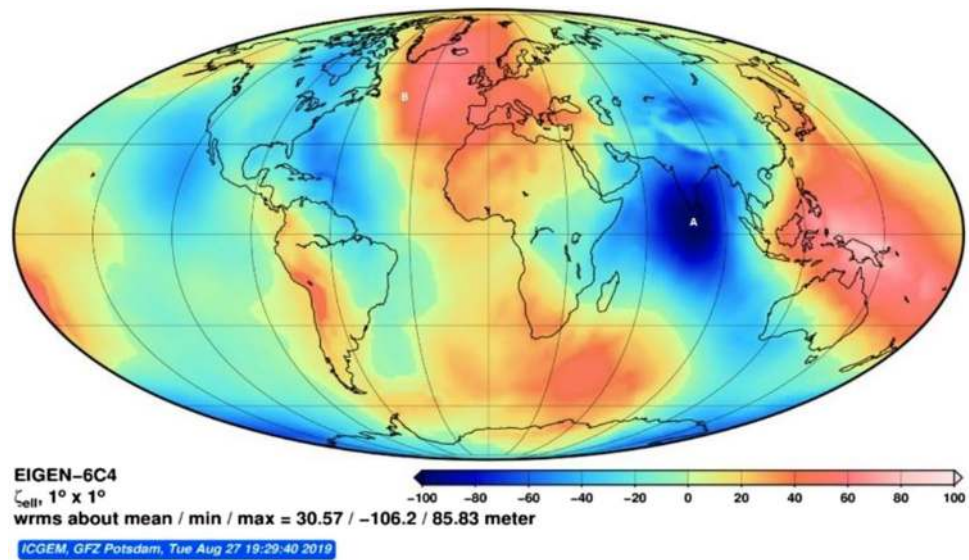
Figure 1. Digital data for EIGEN-6C4 geoid undulation (N) with $1° \times 1°$, computed online at the website http://icgem.gfz-potsdam.de/home.

$$T(\lambda, \varphi, z) \approx T(\lambda, \varphi, 0), \quad 0 \geq z \geq -H(\lambda, \varphi) \tag{13}$$

Since the deviation of the vertical component of the gravity (g_z) to a constant ($-g_0$) is 3–4 orders of magnitude smaller than g_0, it leads to the second approximation

$$g_z \approx -g_0 \tag{14}$$

With the two approximations, the near real gravity in the water column is given by

$$g_x(\lambda, \varphi, z) \approx g_0 \frac{\partial N}{\partial x}, \, g_y(\lambda, \varphi, z) \approx g_0 \frac{\partial N}{\partial y}, \, g_z(\lambda, \varphi, z) \approx -g_0 \tag{15}$$

Correspondingly, the potential of the real gravity is approximately given by

$$V(\lambda, \varphi, z) \approx g_0[N(\lambda, \varphi) - z] \tag{16}$$

where Eq. (9) is used.

Unexpectedly large horizontal gravity component. For simplicity, the local coordinates (x, y, z) are used from now on to replace the polar spherical coordinates with x representing longitude (eastward positive) and y representing latitude (northward positive). The local and spherical coordinate systems are connected by

$$\frac{\partial}{\partial x} = \frac{1}{R \cos \varphi} \frac{\partial}{\partial \lambda}, \frac{\partial}{\partial y} = \frac{1}{R} \frac{\partial}{\partial \varphi}, \, \frac{\partial}{\partial z} = \frac{\partial}{\partial r} \tag{17}$$

The EIGEN-6C4 model[14,15], listed on the website http://icgem.gfz-potsdam.de/home, was developed jointly by the GFZ Potsdam and GRGS Toulouse up to degree and order 2190 to produce global static geoid height (N) dataset. Following the instruction, the author ran the EIGEN-6C4 model in $1° \times 1°$ resolution for 17 s to get the global N (Fig. 1) with mean value of 30.57 m, minimum value of -106.20 m, and maximum of 85.83 m. Two locations on the marine geoid are identified with $N_A = -99.76$ m at A (80° W, 3° N) in the Indian Ocean, and $N_B = 65.38$ m at B (26° W, 45° N) in the North Atlantic Ocean, i.e., $|\Delta N|_{AB} = 165.14$ m. The big circle distance between A and B is about $\Delta L = 7920$ km. Equation (11) shows that the corresponding $|\mathbf{g}_h|$ at z = 0 is computed by

$$\left.\left|\mathbf{g}_h\right|\right|_{AB} = g_0 \frac{|\Delta N|_{AB}}{\Delta L} = 9.81 \text{ m/s}^2 \times \frac{165.14 \text{ m}}{7.920 \times 10^6 \text{ m}} = 20.45 \text{ mGal} \tag{18}$$

With the geoid height data obtained from the EIGEN-6C4, $N(x, y)$, the horizontal gravity components g_x (Fig. 2a) and g_y (Fig. 2b) at z = 0 are computed using Eq. (11). The magnitude of the horizontal gravity vector is calculated by

$$\left|\mathbf{g}_h(x, y)\right| = \sqrt{\left[g_x(x, y)\right]^2 + \left[g_y(x, y)\right]^2}, \tag{19}$$
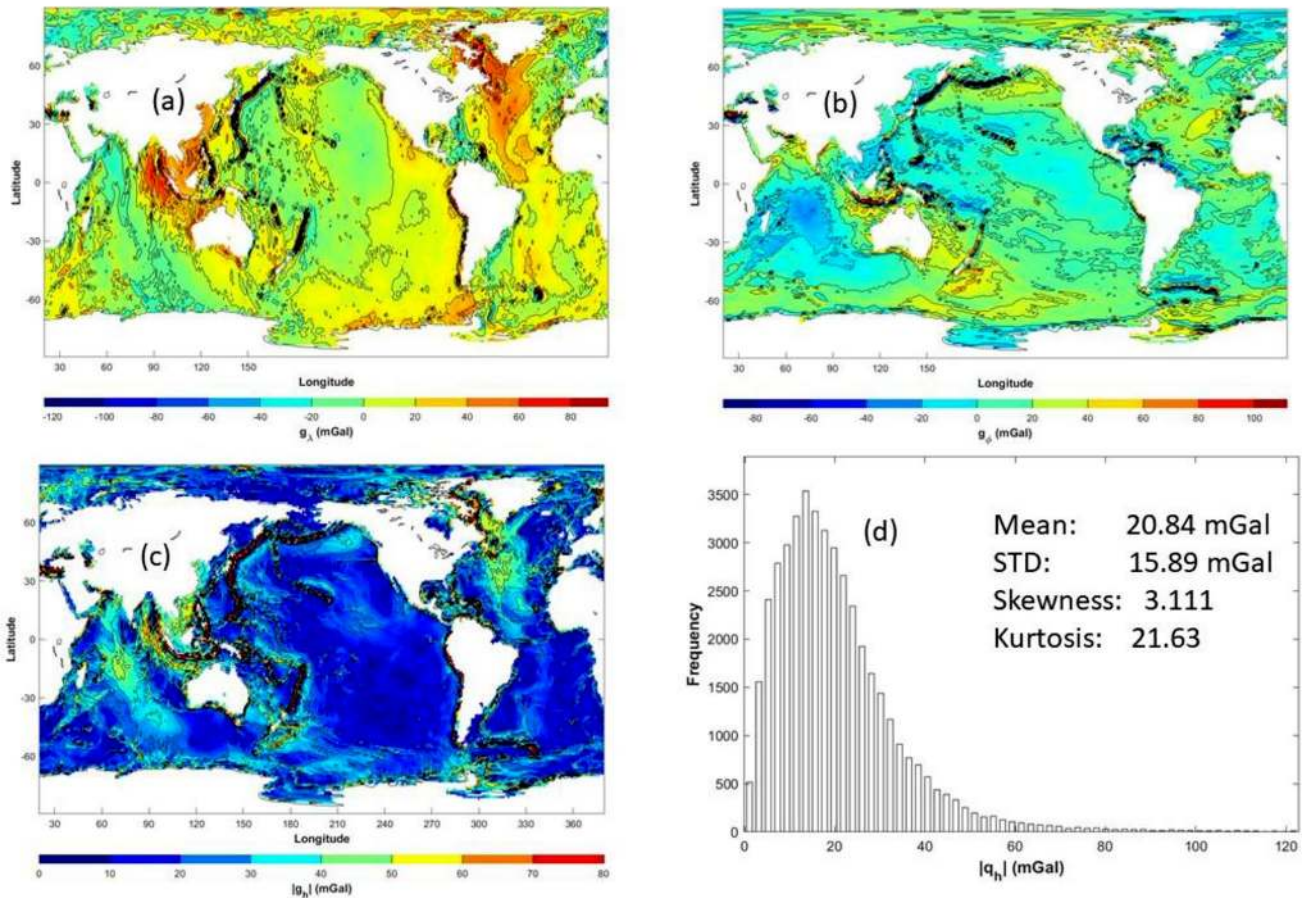
Figure 2. Horizontal gravity components (unit: mGal) at $z = 0$: (**a**) longitudinal component (g_λ), (**b**) latitudinal component (g_φ), (**c**) magnitude of the horizontal gravity vector $|\mathbf{g}_h|$, and (**d**) histogram of $|\mathbf{g}_h|$ (from the reference[16]). The source codes for the plots were written by the author 's research group using the Matlab Version R2019b (https://www.mathworks.com/products/matlab.html).

as shown in Fig. 2c. The histogram of $|\mathbf{g}_h|$ (Fig. 2d) indicates a positively skewed distribution with a long tail extending to values larger than 100 mGal (1 mGal = 10^{-5} m s^{-2}). The statistical characteristics of $|\mathbf{g}_h|$ are 20.84 mGal as the mean, 15.89 mGal as the standard deviation, 3.11 as the skewness, and 21.63 as the kurtosis. The statistical estimate of the mean intensity of the horizontal gravity $|\mathbf{g}_h|$ (20.84 mGal) is coherent with the simple calculation of $|\mathbf{g}_h|_{AB}$ between points A and B (20.45 mGal). The two values (20.84 mGal, 20.45 mGal) are unexpectedly large.

C number to identify importance of the horizontal gravity.   The importance of the horizontal gravity can be identified by a non-dimensional C number[16] from the analysis of horizontal gravity versus the Coriolis force,

$$C(x, y, z) = \frac{|\mathbf{g}_h|}{|f|U} \tag{20}$$

where $f = 2\Omega\sin\varphi$, is the Coriolis parameter; and U is the speed of the horizontal current. With Eq. (11) the C number at $z = 0$ is given by

$$C_0(x, y) \equiv C(x, y, 0) = \frac{g_0|\Delta N|}{|f|U\Delta L} \tag{21}$$

where ΔL is the horizontal scale of the motion.

The Ocean Surface Current Analysis Real-time (OSCAR) third degree resolution 5-day mean surface current vectors[17] on 26 February 2020 (Fig. 3a) was downloaded from the website https://podaac-tools.jpl.nasa.gov/drive/files/allData/oscar/ and the data at the same 1° × 1° grid points as the EIGEN-6C4 data were used. The data represent vertically averaged surface currents over the top 30 m of the upper ocean, which consist of a geostrophic component with a thermal wind adjustment using satellite sea surface height, and temperature and a wind-driven ageostrophic component using satellite surface winds. The histogram of the OSCAR current
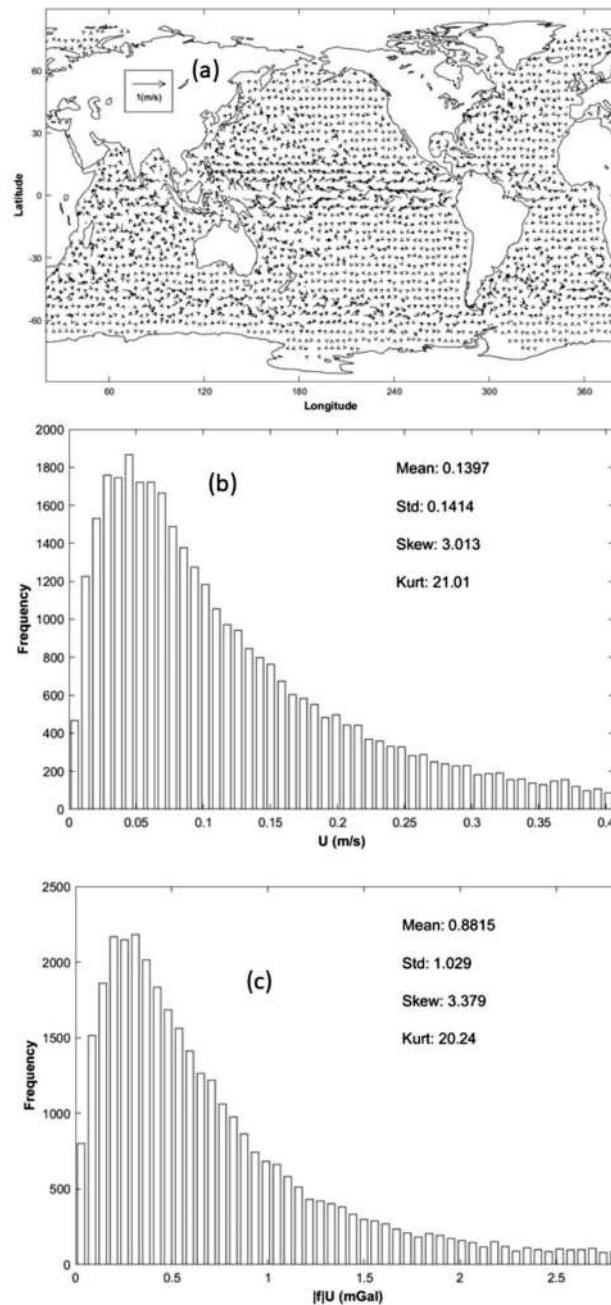
Figure 3. (**a**) The world ocean surface current vectors on 26 February 2020 from the ocean surface current analysis real-time (OSCAR) dataset which was downloaded from the website https://podaac-tools.jpl.nasa.gov/drive/files/allData/oscar/, (**b**) histogram of the current speed U, and (**c**) histogram of the intensity of the Coriolis force $|f|U$. The source codes for the plots were written by the author's research group using the Matlab Version R2019b (https://www.mathworks.com/products/matlab.html).

speed $U(x, y)$ (Fig. 3b) indicates a positively skewed distribution with a long tail extending to values larger than 0.4 m/s. The statistical characteristics of U are 0.1397 m/s as the mean, 0.1414 m/s as the standard deviation, 3.013 as the skewness, and 21.01 as the kurtosis. The histogram of the corresponding Coriolis force $|f|U(x, y)$ (Fig. 3c) also shows a positively skewed distribution with a long tail extending to values larger than 2.5 mGal. The statistical characteristics of $|f|U$ are 0.8815 mGal as the mean, 1.029 mGal as the standard deviation, 3.379 as the skewness, and 20.24 as the kurtosis. Comparison between Figs. 2d and 3c leads to the fact that the mean intensity of horizontal gravity component $|\mathbf{g}_h|$ $(= 20.84$ mGal) is nearly 24 times as large as the mean intensity of the Coriolis force identified from the OSCAR surface currents on 26 February 2020. Such unexpectedly large horizontal gravity component is also shown in the world ocean distribution of $(1/C_0)$ values (Fig. 4a). The histogram of $(1/C_0)$ (Fig. 4b) indicates a positively skewed distribution with a long tail extending to values larger than 0.18. The statistical characteristics of $(1/C_0)$ are 0.04238 as the mean, 0.04108 as the standard deviation, 1.447
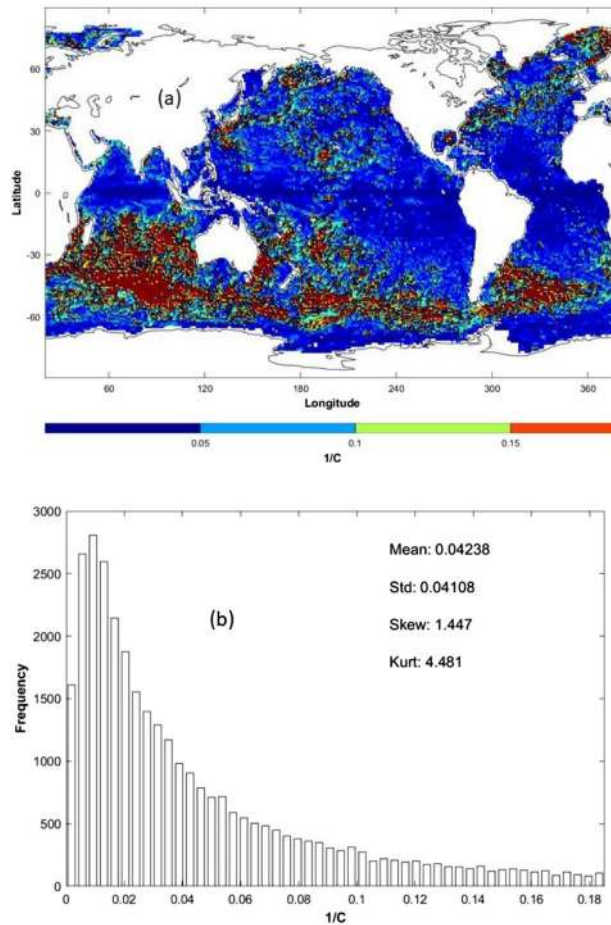
Figure 4. (**a**) The world ocean surface (z = 0) distribution of (1/C), and (**b**) histogram of (1/C). The source codes for the plots were written by the author 's research group using the Matlab Version R2019b (https://www.mathworks.com/products/matlab.html).

as the skewness, and 4.481 as the kurtosis. Thus, the global mean of C_0 is about 23.6, which is coherent with the rough estimate given above using the geoid height data at the two points A and B (near 24).

New equations with the real gravity. Application of the Newton's second law of motion into the ocean for the large-scale motions with the Boussinesq approximation leads to

$$\rho_0 \left[\frac{D\mathbf{U}}{Dt} + 2\mathbf{\Omega} \times \mathbf{U} \right] = -\nabla p + \rho \nabla V + \rho_0 \mathbf{F} \qquad (22)$$

if the pressure gradient force, gravitation, and friction are the only real forces. Here, $\mathbf{\Omega} = \Omega \left(\mathbf{j} \cos \varphi + \mathbf{k} \sin \varphi \right)$, is the Earth rotation vector with $\Omega = 2\pi/(86,400 \text{ s})$ the Earth rotation rate; ρ is the density; $\rho_0 = 1028 \text{ kg/m}^3$, is the characteristic density; $\mathbf{U} = (u, v)$, is the horizontal velocity vector; ∇ is the three dimensional vector differential operator; and D/Dt is the total time rate of change; $\mathbf{F} = (F_x, F_y)$, is the frictional force and usually represented using vertical eddy viscosity K,

$$F_x = \frac{\partial}{\partial z} \left(K \frac{\partial u}{\partial z} \right), \ F_y = \frac{\partial}{\partial z} \left(K \frac{\partial v}{\partial z} \right) \qquad (23)$$

The continuity equation is given by

$$\nabla_h \cdot \mathbf{U} + \frac{\partial w}{\partial z} = 0 \qquad (24)$$

where w is the vertical velocity. Substitution of (16) into (22) leads to

$$\rho_0 \left[\frac{D\mathbf{U}}{Dt} + 2\mathbf{\Omega} \times \mathbf{U} \right] = -\nabla p + \rho g_0 \nabla_h N - g_0 \mathbf{k} + \rho_0 \mathbf{F} \qquad (25)$$

Equation (25) can be easily used by any ocean numerical model with just adding the horizontal gravity component represented by ($\rho g_0 \nabla_h N$).

Hydrostatic balance. Large-scale oceanic motion is hydrostatically balanced,

$$-\frac{\partial p}{\partial z} + \rho \frac{\partial V}{\partial z} = 0 \Rightarrow dp = \rho dV \qquad (26)$$

Vertical integration of this equation from the marine geoid (i.e., $V = 0$) to any equipotential surface V leads to the integral form of the hydrostatic balance

$$p = \int\limits_{-V(x,y,z)}^{0} \rho d\tilde{V} + \rho_0 g_0 (S - N) \qquad (27)$$

where S is the sea surface height; and the marine geoid surface (N) is the coincidence of the equipotential and isobaric surfaces (i.e., balance of the 3D pressure gradient force and gravity on N).

Equipotential (-V) coordinate system. The hydrostatic Eq. (27) clearly shows that a single valued monotonic relationship exists between gravitational potential and the depth in each vertical water column. Thus, we may use (-V) as the independent vertical coordinate. The negative sign is due to the vertical component of the gravity is defined positive downward. The total derivative is expanded as

$$\begin{aligned}
\frac{D}{Dt} &= \frac{\partial}{\partial t} + \frac{Dx}{Dt}\frac{\partial}{\partial x} + \frac{Dy}{Dt}\frac{\partial}{\partial y} + \frac{D(-V)}{Dt}\frac{\partial}{\partial(-V)} \\
&= \frac{\partial}{\partial t} + u\frac{\partial}{\partial x} + v\frac{\partial}{\partial y} + \omega\frac{\partial}{\partial V}
\end{aligned} \qquad (28)$$

The continuity Eq. (24) becomes

$$\nabla_h \cdot \mathbf{U} + \frac{\partial \omega}{\partial V} = 0 \qquad (29)$$

here,

$$\omega \equiv \frac{dV}{dt} = \mathbf{U} \cdot \nabla_h V + w\frac{\partial V}{\partial z} \qquad (30)$$

where ω is the "vertical velocity" in the V-coordinate. Note that V is the static gravitational potential such that $\partial V/\partial t = 0$.

Dynamic equations in the equipotential coordinate system. The horizontal pressure gradients can be computed from (27),

$$\begin{aligned}
\frac{\partial p}{\partial x} &= \rho\frac{\partial V}{\partial x} + \int\limits_{-V}^{0}\frac{\partial \rho}{\partial x}d\tilde{V} + \rho_0 g_0\frac{\partial(S-N)}{\partial x}, \\
\frac{\partial p}{\partial y} &= \rho\frac{\partial V}{\partial y} + \int\limits_{-V}^{0}\frac{\partial \rho}{\partial y}d\tilde{V} + \rho_0 g_0\frac{\partial(S-N)}{\partial y}
\end{aligned} \qquad (31)$$

Substitution of (31) into (22) leads to the horizontal momentum equations

$$\frac{Du}{Dt} - fv = -\frac{1}{\rho_0}\int\limits_{-V}^{0}\frac{\partial \rho}{\partial x}d\tilde{V} - g_0\frac{\partial(S-N)}{\partial x} + F_x \qquad (32a)$$

$$\frac{Dv}{Dt} + fu = -\frac{1}{\rho_0}\int\limits_{-V}^{0}\frac{\partial \rho}{\partial y}d\tilde{V} - g_0\frac{\partial(S-N)}{\partial y} + F_y \qquad (32b)$$

Extended geostrophic equilibrium and thermal wind relation. For steady state (no total derivative) without friction, Eqs. (32a) and (32b) become the extended equations for the geostrophic currents

$$-fv_G = -\frac{1}{\rho_0}\int\limits_{-V}^{0}\frac{\partial \rho}{\partial x}d\tilde{V} - g_0\frac{\partial(S-N)}{\partial x} \qquad (33a)$$

$$fu_G = -\frac{1}{\rho_0}\int\limits_{-V}^{0}\frac{\partial\rho}{\partial y}d\tilde{V} - g_0\frac{\partial(S-N)}{\partial y} \tag{33b}$$

Vertical derivative of (33a) and (33b) leads to the extended thermal wind relation

$$-f\frac{\partial v_G}{\partial z} = \frac{g_0}{\rho_0}\frac{\partial\rho}{\partial x} - \frac{1}{\rho_0}\int\limits_{-V}^{0}\frac{\partial^2\rho}{\partial x\partial z}d\tilde{V} \tag{34a}$$

$$f\frac{\partial u_G}{\partial z} = \frac{g_0}{\rho_0}\frac{\partial\rho}{\partial y} - \frac{1}{\rho_0}\int\limits_{-V}^{0}\frac{\partial^2\rho}{\partial y\partial z}d\tilde{V} \tag{34b}$$

where the vertical differentiation of lower limit (-V) of the integrals of the righthand side of (33a) and (33b)

$$\frac{\partial V}{\partial z} = g_z \approx -g_0 \tag{35}$$

is used.

Vorticity equation.   Subtraction of the differentiation of the longitudinal component of Eq. (25) with respect to y from the differentiation of the latitudinal component of Eq. (25) with respect to x leads to the vorticity equation,

$$\frac{\partial\zeta}{\partial t} = -\mathbf{U}\cdot\nabla_h\zeta - \omega\frac{\partial\zeta}{\partial V} + \beta v - (\zeta+f)\nabla_h\cdot\mathbf{U} + \mathbf{k}\cdot\left(\frac{\partial\mathbf{U}}{\partial V}\times\nabla_h\omega\right)$$
$$+ \frac{g_0}{\rho_0}J(\rho,N) + \left(\frac{\partial F_y}{\partial x} - \frac{\partial F_x}{\partial y}\right) \tag{36}$$

where $J(\rho,N) = (\partial\rho/\partial x)(\partial N/\partial y) - (\partial\rho/\partial y)(\partial N/\partial x)$, is the Jacobian; $\beta = df/dy$ is the latitudinal change of the Coriolis parameter; and $\zeta = \partial v/\partial x - \partial u/\partial y$ is the vertical vorticity.

Conclusion
The non-dimensional C number is used to identify relative importance of the horizontal gravity and the Coriolis force using the geoid height data (N) provided by the EIGEN-6C4 gravity model, and the Ocean Surface Current Analysis Real-time (OSCAR) surface current vectors on 26 February 2020. Unexpectedly large value of the C number (global mean around 24) may surprise both oceanographic and geodetic communities. It is very hard for my oceanographic colleagues to accept such strong horizontal gravity (at $z = 0$), which is an order of magnitude lager that the Coriolis force. Thus, in situ measurement of gravity may be needed for oceanography in addition to the routine hydrographic and current meter measurements.

A geodesist may also be surprised that the horizontal gravity ($z = 0$) associated with the geoid height (N) varying between -106.20 m to 85.83 m (well accepted by the geodetic community), which was produced by a community gravity model (EIGEN-64C), generates the ocean currents with the intensity nearly 24 times as large as the currents identified from the ocean surface current analysis real-time (OSCAR) (oceanographic community product).

How to resolve such incoherency between the two communities on this issue becomes urgent. The new ocean dynamic equations including the horizontal gravity may provide a theoretical framework to resolve the incoherency since the potential of the real gravity (V) obtained from a geodetic gravity model is explicitly in the dynamical equations. Besides, use of the real gravity in the ocean dynamics may ultimately resolve some fundamental problems in oceanography such as reference level, and absolute geostrophic current calculation. A new dynamic system for large-scale oceanic motion with the real gravity is presented such as hydrostatic balance, geostrophic equilibrium, thermal wind, equipotential coordinate system, and the vorticity equation. Close collaboration between the oceanographic and geodetic communities helps the use of the real gravity in oceanography and the verification of the gravity model in geodesy with oceanographic data.

Appendix: Oblate spheroid coordinates versus polar spherical coordinates
This paper uses the polar spherical coordinates rather than the oblate spheroid coordinates for computational simplicity with a small error (0.17%)[18]. The oblate spheroid coordinates share the same longitude (λ) but different latitude (φ_{ob}) and radial coordinate (representing vertical) (r_{ob}). The relationship between the oblate spheroid coordinates (λ, φ_{ob}, r_{ob}) and the polar spherical coordinates (λ, φ, r) is given by[18]

$$r^2 = r_{ob}^2 + \frac{1}{2}d^2 - d^2\sin^2\varphi_{ob}, \quad r^2\cos^2\varphi = (r_{ob}^2 + \frac{1}{2}d^2)\cos^2\varphi_{ob} \tag{37}$$

where d is the half distance between the two foci of the ellipsoid. For the normal Earth, $d = 521.854$ km. The vector differential operator in the oblate spheroid coordinates is represented by

$$\nabla = \mathbf{i}\frac{1}{h_\lambda^{ob}}\frac{\partial}{\partial\lambda} + \mathbf{j}\frac{1}{h_\varphi^{ob}}\frac{\partial}{\partial\varphi} + \mathbf{k}\frac{1}{h_r^{ob}}\frac{\partial}{\partial z}, \quad z = r - R \tag{38}$$

where $R = 6.3781364 \times 10^6$ m, is the semi-major axis of the normal Earth (Earth radius). The coefficients (h_λ^{ob}, h_φ^{ob}, h_r^{ob}) are given by

$$h_\lambda^{ob} = \sqrt{r^2 + \frac{1}{2}d^2}\cos\varphi, \ h_\varphi^{ob} = \sqrt{r^2 - \frac{1}{2}d^2 + d^2\sin^2\varphi}, \ h_r^{ob} = \frac{r\sqrt{r^2 - \frac{1}{2}d^2 + d^2\sin^2\varphi}}{\sqrt{r^4 - \frac{1}{4}d^4}}. \tag{39}$$

However, the vector differential operator in the polar spherical coordinates is represented by

$$\nabla = \mathbf{i}\frac{1}{r\cos\varphi}\frac{\partial}{\partial\lambda} + \mathbf{j}\frac{1}{r}\frac{\partial}{\partial\varphi} + \mathbf{k}\frac{\partial}{\partial z}. \tag{40}$$

References

1. Sun, F., Kim, V. S., Huang, B. & Wang, D. Water exchange between the subpolar and subtropical North Pacific Ocean in an OGCM. *Sci. China D* **47**, 37–48 (2004).
2. Chu, P. C., Fan, C. W. & Cai, W. J. P vector method evaluated using modular ocean model (MOM). *J. Oceanogr.* **54**, 185–198 (1998).
3. Wang, D., Wang, J. & Wu, L. Regime shifts in the North Pacific simulated by a COADS-driven isopycnal model. *Adv. Atmosph. Sci.* **20**, 743–754 (2003).
4. Chu, P. C. & Li, R. F. South China Sea isopycnal surface circulations. *J. Phys. Oceanogr.* **30**, 2419–2438 (2000).
5. Chu, P. C. & Fan, C. W. Sixth-order difference scheme for sigma coordinate ocean models. *J. Phys. Oceanogr.* **27**, 2064–2071 (1997).
6. Chu, P. C., Lu, S. H. & Chen, Y. C. Evaluation of the Princeton Ocean model using the South China Sea Monsoon experiment (SCSMEX) data. *J. Atmos. Oceanic Technol.* **18**, 1521–1539 (2001).
7. Vaniček, P. & Krakiwsky, E. *Geodesy: The Concepts* 697 (North-Holland, Amsterdam, 1986).
8. National Geospatial-Intelligence Agency. *Department of Defense World Geodetic System 1984 (WGS84).* Its definition and relationships with local geodetic systems. NIMA TR8350.2., 3rd Edition, Equation 4–1 (1984).
9. Hackney, R. I. & Featherstone, W. E. Geodetic versus geophysical perspectives of the 'gravity anomaly'. *Geophys. J. Int.* **154**, 35–43 (2003).
10. Sandwell, D. T. & Smith, W. H. F. Marine gravity anomaly from Geosat and ERS 1 satellite altimetry. *J. Geophys. Res.* **102**(B5), 10039–10054 (1997).
11. Kostelecký, J., Klokočnìk, J., Bucha, B., Bezděk, A. & Förste, C. Evaluation of the gravity model EIGEN-6C4 in comparison with EGM2008 by means of various functions of the gravity potential and by BNSS/levelling. *Geoinform. FCE CTU.* https://doi.org/10.14311/gi.14.1.1 (2015).
12. Chu, P. C. Two types of absolute dynamic ocean topography. *Ocean Sci.* **14**, 947–957 (2018).
13. Chu, P. C. A. Complete formula of ocean surface absolute geostrophic current. *Nat. Sci. Rep,* **10**, Article number 1445 (2020).
14. Ince, E. S. *et al.* ICGEM: 15 years of successful collection and distribution of global gravitational models, associated services, and future plans. *Earth Syst. Sci. Data* **11**, 647–674 (2019).
15. Förste, C., Bruinsma, S.L., Abrikosov, O., Lemoine, J.M., Marty, J.C., Flechtner, F., Balmino, G., Barthelmes, F., & Biancale, R. EIGEN-6C4. The latest combined global gravity field model including GOCE data up to degree and order 2190 of GFZ Potsdam and GRGS Toulouse, https://doi.org/10.5880/icgem.2015.1 (2014).
16. Chu, P. C. Occurrence of spurious geostrophic currents on the marine geoid without horizontal gravity component. *Nat. Sci. Rep,* in press (2020).
17. ESR. OSCAR third deg. ver. 1. PO.DAAC, CA, USA. Dataset accessed [2020-11-10] at https://doi.org/10.5067/OSCAR-03D01 (2009).
18. Gill, A. E. *Atmosphere-Ocean Dynamics. International Geophysics Series* Vol. 30, 91–94 (Academic Press, New York, 1982).

Author contributions

P.C.C. designed the project, obtained the datasets, conducted the computation, and wrote the manuscript.

Competing interests

The author declares no competing interests.

Additional information

Correspondence and requests for materials should be addressed to P.C.C.

Reprints and permissions information is available at www.nature.com/reprints.

Publisher's note Springer Nature remains neutral with regard to jurisdictional claims in published maps and institutional affiliations.